Mon. Not. R. Astron. Soc. **000**, 1–5 (2002) Printed 25 July 2002 (MN LATEX style file v2.2)

Intrinsic correlation of halo ellipticity and its implications for large-scale weak lensing surveys

Y.P. Jing[1,2⋆]
[1] *Shanghai Astronomical Observatory, the Partner Group of Max-Planck Institut für Astrophysik, Nandan Road 80, Shanghai 200030, China*
[2] *Beijing Astrophysics Center and Department of Astronomy, Peking University, 100871 Beijing, China*

Accepted ???. Received ???

ABSTRACT

We use a large set of state-of-the-art cosmological N-body simulations [512^3 particles] to study the intrinsic ellipticity correlation functions of halos. With the simulations of different resolutions, we find that the ellipticity correlations converge once the halos have more than 160 members. For halos with fewer members, the correlations are underestimated, and the underestimation amounts to a factor of 2 when the halos have only 20 particles. After correcting for the resolution effects, we show that the ellipticity correlations of halos in the bigger box ($L = 300\,h^{-1}$Mpc) agree very well with those obtained in the smaller box ($L = 100\,h^{-1}$Mpc). Combining these results from the different simulation boxes, we present accurate fitting formulae for the ellipticity correlation function $c_{11}(r)$ and for the projected correlation functions $\Sigma_{11}(r_p)$ and $\Sigma_{22}(r_p)$ over three orders of magnitude in halo mass. The latter two functions are useful for predicting the contribution of the intrinsic correlations to deep lensing surveys. With reasonable assumptions for the redshift distribution of galaxies and for the mass of galaxies, we find that the intrinsic ellipticity correlation can contribute significantly not only to shallow surveys but also to deep surveys. Our results indicate that previous similar studies significantly underestimated this contribution for their limited simulation resolutions.

Key words: Cosmology: theory — cosmology: observations — gravitational lensing — large-scale structure of universe — dark matter

1 INTRODUCTION

Inhomogeneities of matter distribution in the Universe distort the images of distant galaxies gravitationally, a phenomenon called gravitational lensing. The lensing effect induces an ellipticity-ellipticity correlation of the galaxies on large scales, which is observable and can be used as a powerful tool to probe the large-scale dark matter distribution in the Universe (Miralda-Escude 1991; Blandford et al. 1991; Kaiser 1992; see Bartelmann & Schneider 2001 and Mellier 1999 for reviews). Several groups have already detected the ellipticity correlation on scales from 0.4 to 30 arc-minutes for faint galaxies (Bacon et al. 2000, 2002; Hoekstra et al. 2002a,b; Kaiser et al. 2000; Maoli et al. 2001,; Rhodes et al. 2000, 2001; van Waerbeke et al. 2000, 2001; Wittman et al. 2000). If the source galaxies are randomly oriented without the lensing effect, that is, the intrinsic ellipticity correlation of the galaxies is negligible, the observed ellipticity correlation implies that the parameter $\beta \equiv \Omega_0^{0.6}\sigma_8$ is about 0.6, where Ω_0 is the density parameter, σ_8 is the current rms linear density fluctuation in a top-hat sphere of $8\,h^{-1}$Mpc, and h is the Hubble constant in units of 100km s^{-1}Mpc^{-1}.

There are however evidences both from theory and from observations that the shapes of galaxies are intrinsically correlated. In the theory, the large scale tidal field is expected to induce large-scale correlations in galaxy spins and in galaxy shapes (Lee & Pen 2000, 2001; Croft & Metzler 2000, hereafter CM00; Heavens et al. 2000, hereafter HRH00; Catelan et al. 2001; Catelan & Porciani 2001; Hui & Zhang 2002; Porciani et al. 2002). It is recently claimed that a large-scale alignment of galaxy spins has been detected in nearby galaxy catalogs with a high confidence (Pen et al. 2000, Lee & Pen 2002; Brown et al. 2002; Plionis 1994 for cluster shapes). While the intrinsic ellipticity correlation may be separated from the weak lensing signal in observations through measuring the E-mode and the B-mode correlations of the ellipticity (Crittenden et al. 2001, Mackey et al. 2002), applying this technique needs an accurate relation between the E-mode and B-mode correlations (Crittenden et al. 2001, 2002; Pen et al. 2002; Schneider et al. 2002; Hoekstra et al. 2002b). In this aspect, the current situations are far from satisfactory, since there are still considerable uncertainties

⋆ E-mail: ypjing@center.shao.ac.cn

both in the theoretical predictions and in the observational measurements of the intrinsic ellipticity correlations.

Using the numerical simulations of 256^3 particles released by the Virgo Consortium, HRH00 and CM00 measured the ellipticity correlation for dark matter halos and discussed their results in the context of weak lensing measurements[1]. Assuming that the galaxies have the same intrinsic correlations as their host halos, they found that the intrinsic correlation of galaxy ellipticity could dominate over the lensing signal in shallow lensing surveys, and could contribute a non-negligible signal, as high as 20 percent, to deep lensing surveys like those that reported detections of the weak lensing effects. Their findings already have profound implications for interpreting the weak lensing experiments, but quantitatively speaking, there are still significant uncertainties in their results. For examples, CM00 compared the ellipticity correlation $c_{11}(r)$ for halos of a mass $> 1.4 \times 10^{12}h^{-1}\mathrm{M}_\odot$ between two simulations of boxsizes $L = 141\,h^{-1}$Mpc and $240\,h^{-1}$Mpc, and found that $c_{11}(r)$ in the higher resolution simulation ($L = 141\,h^{-1}$Mpc) is $2 \sim 3$ times higher. The ellipticity correlation $c_{11}(r)$ found in CM00 is also a factor of 2 or more higher than that found in HRH00. Therefore, it is unclear how their selections of halos and simulation resolutions have affected their results.

In this *Letter*, we will first quantify how the simulation resolution affects the determination of the ellipticity correlation using a set of state-of-the-art cosmological N-body simulations of 512^3 particles (Jing & Suto 2002) and a set of lower-resolution simulations of 256^3 particles (Jing 1998; Jing & Suto 1998). We will show that the minimum particle number $N_{\rm min}$ for resolving the halo shapes in simulations is 160, and the ellipticity correlation functions of halos with more than $N_{\rm min}$ particles are well converged. We will also show that the ellipticity correlation is underestimated by a factor 2 when halos of about twenty particles are used. Therefore, the predictions of CM00 and HRH00 for weak lensing surveys are significantly underestimated, since the halos of ten (HRH00) or twenty (CM00) particles were included in their studies (in order to have a sufficient number of halos for their analyses). Our results imply that the intrinsic ellipticity correlation may have a significant contribution even to deep weak lensing surveys. Our simulations are also large enough for accurately measuring the scale- and mass-dependences of the ellipticity correlation functions. Based on the simulation data, accurate fitting formulae are presented for these functions. These formulae can be used to predict the intrinsic ellipticity signals, including E-mode and B-mode contributions, in large-scale lensing surveys (Crittenden et al. 2001, 2002; Schneider et al. 2001; Pen et al. 2002).

In the next section, we will measure the ellipticity correlation functions in a set of N-body simulations, and will do the convergence test. In Section 3, we will present the projected ellipticity correlation functions, which are useful for predicting the intrinsic ellipticity contribution in weak lensing surveys once the radial (or redshift) distribution of source galaxies is known. Our results are summarized and discussed in Section 4.

[1] HRH00 also examined the correlation of the halo spins.

Table 1. Cosmological N-body simulations

$L[h^{-1}\mathrm{Mpc}]$	N_p	σ_8	$m_p[h^{-1}\mathrm{M}_\odot]$	realizations
100	512^3	0.9	6.2×10^8	4
300	512^3	0.9	1.7×10^{10}	4
100	256^3	1.0	5.0×10^9	3

2 THE ELLIPTICITY CORRELATION FUNCTIONS OF HALOS

We use a set of cosmological N-body simulations of 512^3 particles that are listed in Table 1. The cosmological model is a currently popular flat low-density model with the density parameter $\Omega_0 = 0.3$ and the cosmological constant $\lambda_0 = 0.7$ (LCDM). The shape parameter $\Gamma = \Omega_0 h$ and the amplitude σ_8 of the linear density power spectrum respectively are 0.2 and 0.9. Two different boxsizes $L = 100\,h^{-1}$Mpc and $L = 300\,h^{-1}$Mpc are adopted, and the particle mass m_p is $6.2 \times 10^8 h^{-1}\mathrm{M}_\odot$ and $1.7 \times 10^{10}h^{-1}\mathrm{M}_\odot$ respectively in these two cases. Thus, halos of galactic sizes are well resolved in both types of simulations. The simulation data were generated on the VPP5000 Fujitsu supercomputer of the National Astronomical Observatory of Japan with our vectorized-parallel P^{3}M code (Jing & Suto 2002), and those of $L = 100\,h^{-1}$Mpc have already been used by Jing & Suto (2002) to derive a tri-axial model for density profiles of halos which is significantly more accurate than the conventional spherical model. There are 4 realizations for each boxsize. For comparison, we use three realizations of our previous N-body simulations for the LCDM model that contains 256^3 particles (Jing & Suto 1998; Jing 1998). These simulations have the same initial fluctuation phases as the first three realizations of 512^3 particles and $L = 100\,h^{-1}$Mpc, but the normalization $\sigma_8 = 1.0$ in the lower-resolution simulations is slightly higher. We refer readers to Jing & Suto (2002) for complementary information about the simulations.

Dark matter halos are identified with the friends-of-friends method (FOF). A linking length b equal to 0.1 of the mean particle separation is adopted. This linking length is smaller than the nominal value 0.2. The regions selected $b = 0.2$ have a mean density contrast about 180 (Porciani et al. 2002), which approximately correspond to virialized halos. The objects identified with $b = 0.1$ have a mean over-density 8 times higher, and they are actually the inner regions of virialized halos (i.e. regions within about one third of the virial radius). Since we are interested in the ellipticity correlation of galaxies and the galaxies lie in the inner regions of halos, $b = 0.1$ might be more appropriate for our study (see also CM00). The simulation outputs at redshift $z = 1$ are used, for galaxies in deep lensing surveys are at this redshift. We measure the ellipticity correlations that are defined (e.g., Miralda-Escude 1991; HRH00; CM00) as

$$c_{ij}(\mathbf{r}) =< e_i(\mathbf{x})e_j(\mathbf{x}+\mathbf{r}) > \qquad (1)$$

where i and j runs over 1 and 2, and $\mathbf{r}$ is the three dimensional vector connecting a pair of halos. The ellipticity e_1 and e_2 for the halos are defined in a projected plane, say, x-y plane, and are computed with respect to the axes that are parallel and orthogonal to the line joining the two halos in the projected plane. Thus, the ellipticity component e_1 (e_2) corresponds to the elongation and compression along

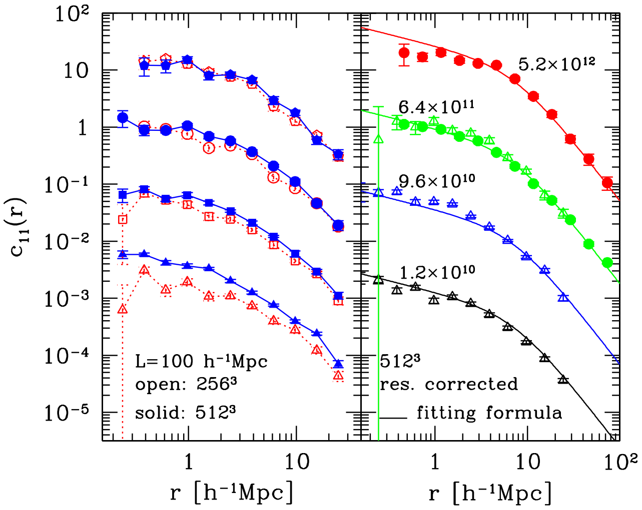

Figure 1. Ellipticity correlation functions of halos $c_{11}(r)$ as a function of the pair separation r. For the clarity, the results for different halo mass, from bottom to top, are multiplied by a factor of 1, 10, 10^2 and 10^3 respectively. *left panel*— The results are presented for the halos of same spatial number density in the simulations of 256^3 particles (open symbols connected with dotted lines) and in the simulations of 512^3 particles (solid symbols connected with solid symbols). From bottom to top, the halos have at least 20, 40, 80, and 160 particles respectively in the lower resolution simulations, and have 7 times more particles in the higher resolution ones (not 8 times because σ_8 is slightly smaller in the latter). *right panels*— A few typical examples for the ellipticity correlation functions $c_{11}(r)$ measured in the simulations of 512^3 particles in the boxes of $100\,h^{-1}$Mpc (open triangles) and of $300\,h^{-1}$Mpc (solid circles). The halos more massive than M_h are included in the analysis, and the values of M_h (in $h^{-1}\mathrm{M}_\odot$) are indicated in the figure. The solid line is our fitting formula (2). The resolution effect has been corrected according to the left panel.

(at 45° from) the line joining the two halos in the projected plane. For each sample of simulations, we compute the correlation functions for the three projections along the x-, y- and z-axes, and consider these projections as independent when estimating the errors.

Our results confirmed that the cross-correlations $c_{21}(\mathbf{r})$ and $c_{12}(\mathbf{r})$ vanish within the measurement errors (HRH00, CM00), and these functions will not be discussed anymore. As found in the previous studies (CM00), we find that the correlation $c_{22}(\mathbf{r})$ is very anisotropic, but $c_{11}(\mathbf{r})$ is nearly isotropic. For the presentation convenience, we will discuss the resolution effect in terms of $c_{11}(r)$.

We analyze $c_{11}(r)$ for halos with particles more than $N_{\rm min}$ in the simulations of 256^3 particles and of 512^3 particles. The simulation box L is $100\,h^{-1}$Mpc, and only the first three realizations are used for $N_p = 512^3$ (so that the random phases of the initial fluctuations are the same in the two sets of the simulations). We consider halos with particles more than $N_{\rm min} = 20$, 40, 80, and 160 in the $N_p = 256^3$ simulations. Since σ_8 is slightly lower in the $N_p = 512^3$ simulations, we fix the corresponding values of $N_{\rm min}$ for this set of simulations by requiring that the halos have the same number density $n(> N_{\rm min})$, and we found $N_{\rm min} = 135$, 270, 540, and 1080. The results are compared in the left panel of Fig.1, which shows that the correlation function is generally underestimated in the lower resolution simulations. The underestimation could be caused by an underestimation of the halo ellipticity and/or a poor determination of the halo orientations in the lower resolution simulations. We found that the latter might be the dominant cause, since the mean ellipticity of halos in the lower resolution simulations are found to be slightly higher ($< 10\%$) than those in the higher resolution simulations. Nonetheless, the statistical results converge very rapidly with the resolution of the halos, and $N_{\rm min} = 160$ is sufficient for the simulation measurement. From this test, we found that the ellipticity correlation is underestimated by a factor of 2.0, 1.5, 1.25 and 1.05 for $N_{\rm min} = 20$, 40, 80, and 160. These resolution effects are also confirmed when we compare the correlation functions from the simulations of different boxsizes with $N_p = 512^3$.

A few examples for $c_{11}(r)$ measured in our simulations of $N_p = 512^3$ are presented in the right panel of Fig. 1, illustrating for halos spanning over 2 orders of magnitude in mass. The shapes of $c_{11}(r)$ are very similar for different halo mass, and $c_{11}(r; \geqslant M_h)$ for halos with a mass greater than M_h can be well fitted by

$$c_{11}(r; \geqslant M_h) = \frac{3.6 \times 10^{-2} (\frac{M_h}{10^{10} h^{-1} \mathrm{M}_\odot})^{0.5}}{r^{0.4}(7.5^{1.7} + r^{1.7})} \tag{2}$$

which are shown in solid lines in the right panel of Fig.1, where r is in units of h^{-1}Mpc. The results for the two different boxsizes agree very well, as shown by the halos of $M_h = 6.4 \times 10^{11} h^{-1}\mathrm{M}_\odot$ (the second from top) in the figure. For the most massive halos $M_h = 5.2 \times 10^{12} h^{-1}\mathrm{M}_\odot$, the correlation function appears to be slightly flatter than the fitting formula at small separation $r < 1\,h^{-1}$Mpc, though the discrepancy is small considering the errorbars of the simulation data. Here M_h is the mass of FOF groups with $b = 0.1$, which is about half of the nominal virial mass of $b = 0.2$ for typical CDM halos.

3 THE PROJECTED ELLIPTICITY CORRELATION FUNCTIONS

The angular ellipticity correlation functions $C_{ij}(\theta)$, as measured in weak lensing surveys, are related to the three dimensional correlations $e_{ij}(\mathbf{r})$ through a modified Limber's equation (CM00, HRH00),

$$C_{ij}(\theta) = \frac{\int r_1^2 \phi(r_1) r_2^2 \phi(r_2) dr_1 dr_2 [1 + \xi(r_{12})] c_{ij}(r_p, \pi)}{\int r_1^2 \phi(r_1) r_2^2 \phi(r_2) dr_1 dr_2 [1 + \xi(r_{12})]} \tag{3}$$

where r_{12} is the comoving separation between the two galaxies at r_1 and r_2, and r_p and π are the comoving separations perpendicular to and along the line-of-sight. $\xi(r)$ is the two-point correlation function, and $\phi(r)$ is the selection function of a survey. For the flat Universe considered in this paper and at the small-angle limit (i.e. $\theta \ll 1$ which holds well in large-scale lensing surveys), we have,

$$r_p = \frac{r_1 + r_2}{2}\theta, \qquad \pi = r_1 - r_2\,. \tag{4}$$

Since the correlations $e_{ij}(\mathbf{r})$ decrease rapidly at scales $r \geqslant 10\,h^{-1}$Mpc and the selection function $\phi(r)$ changes much more gently on such scales, equation(3) can simplified to

$$C_{ij}(\theta) = \frac{\int r^4 \phi^2(r) dr \Sigma_{ij}(r\theta)}{[\int r^2 \phi(r) dr]^2 + \int r^4 \phi^2(r) dr \int d\pi \xi(r\theta, \pi)} \tag{5}$$

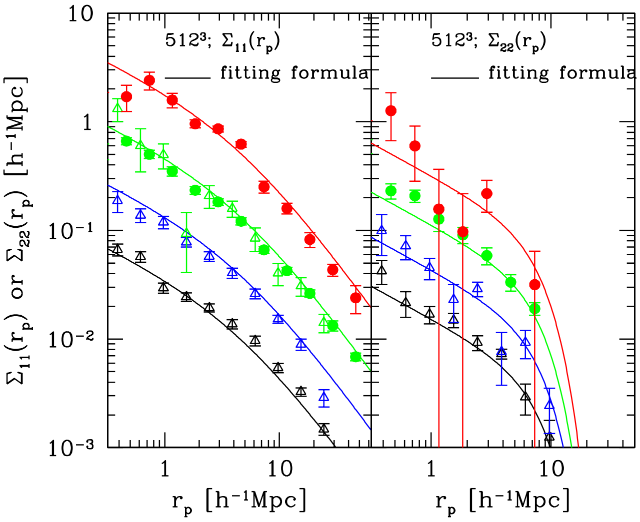

Figure 2. The projected ellipticity correlation functions $\Sigma_{11}(r_p)$ and $\Sigma_{22}(r_p)$ (defined by eq.6) of halos as a function of the project halo separation r_p. The halos are selected and the results are presented in the same way as in the right panel of Fig. 1, but no vertical shifts are made for different halos in this plot. The solid curves are given by fitting formulae (7) and (8) respectively for the left and right panels.

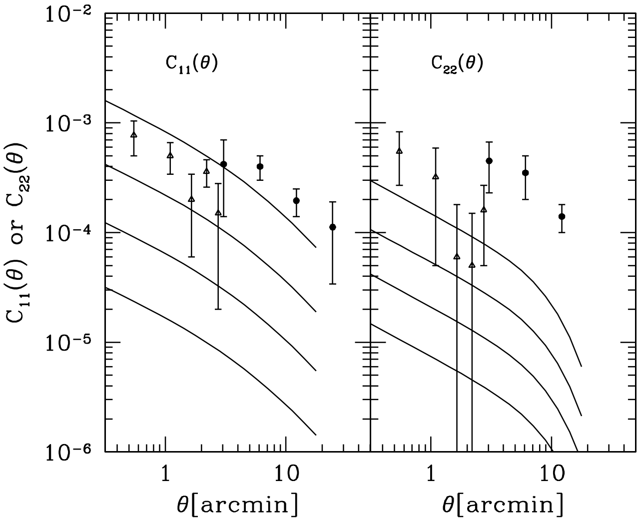

Figure 3. Predictions for the angular ellipticity correlation functions for halos of mass larger than 1.2×10^{10}, 9.6×10^{10}, 6.4×10^{11}, and $5.2\times10^{12}h^{-1}\mathrm{M}_\odot$ (from bottom to top), assuming the source redshift distribution has a median redshift 1. For comparison, the observational data from deep lensing surveys of Van Waerbeke et al. (2000; open triangles) and of Wittman et al. (2000; solid symbols) are plotted.

where we define $\Sigma_{ij}(r_p)$ as

$$\Sigma_{ij}(r_p) \equiv \int d\pi[1+\xi(r_p,\pi)]c_{ij}(r_p,\pi)\,. \tag{6}$$

which we call the projected ellipticity correlation function. This function can be measured directly in the simulations. There are at least two advantages for adopting $\Sigma_{ij}(r_p)$. First, the three-dimensional correlations $c_{ij}(\mathbf{r})$ are generally anisotropic (in fact c_{22} is strongly anisotropic, see CM00), thus it is easier and more accurate to measure the projected functions. Second, more importantly, the projected ellipticity correlations contain all the information needed for predicting the angular correlation functions $C_{ij}(\theta)$ analytically (Eq. 5) once the redshift distribution of source galaxies is known. .

We plot the projected ellipticity correlation functions $\Sigma_{11}(r_p)$ and $\Sigma_{22}(r_p)$ measured from our simulations of 512^3 particles. The halos have correspondingly the same mass as those in the right panel of Fig. 1, and the resolution effects are corrected simply by multiplying the underestimation factors obtained from the convergence test (the left panel of Fig. 1). We find that the results from the two simulation boxes agree very well. The functions $\Sigma_{11}(r_p;\geqslant M_h)$ and $\Sigma_{22}(r_p;\geqslant M_h)$ for halos with mass larger than M_h can be accurately fitted by the following expressions,

$$\Sigma_{11}(r_p;\geqslant M_h) = \frac{0.18(\frac{M_h}{10^{10}h^{-1}\mathrm{M}_\odot})^{0.65}}{r_p^{0.5}(r_p+5)}\,h^{-1}\mathrm{Mpc} \tag{7}$$

$$\Sigma_{22}(r_p;\geqslant M_h) = \frac{1.4\times10^{-2}(\frac{M_h}{10^{10}h^{-1}\mathrm{M}_\odot})^{0.50}}{r_p^{0.6}\exp[\frac{1}{2}(\frac{r_p}{6})^2]}\,h^{-1}\mathrm{Mpc} \tag{8}$$

where r_p is in units of h^{-1}Mpc. We note that from the figure, the readers may get an impression that our fitting formula underestimates Σ_{22} for the most massive halos ($M_h = 5.2\times10^{12}h^{-1}\mathrm{M}_\odot$). But this impression is caused largely by the fact that the two simulation data points at $r_p = 1.2$ and $1.9\,h^{-1}$Mpc, which are significantly smaller than the fitting formula, may be mistakingly considered as those of the less massive halos of $M_h = 6.4\times10^{11}h^{-1}\mathrm{M}_\odot$.

Van Waerbeke et al. (2000) and Wittman et al. (2000) have published their measurements for the angular correlation functions $C_{11}(\theta)$ and $C_{22}(\theta)$ from their deep surveys. Our projected functions can be used to predict the contributions of the intrinsic correlations to these surveys, if it is assumed that the galaxies have the same ellipticity as their host halos. We consider a redshift distribution function

$$p(z) = \frac{\beta}{\Gamma(\frac{1+\alpha}{\beta})}(\frac{z}{z_s})^\alpha \exp[-(\frac{z}{z_s})^\beta] \tag{9}$$

which approximately describes the deep surveys with $\alpha = 2$, $\beta = 1.5$ and $z_s \approx 0.7$ (e.g. Smail et al. 1995; Wittman et al. 2000). Our predictions for the angular correlation functions, based on our fitting formulae for $\Sigma_{11}(r_p;\geqslant M_h)$ and $\Sigma_{22}(r_p;\geqslant M_h)$ and the fitting formula of Jing (1998) for $\xi(r)$ of halos, are shown in Fig. 3, where halo mass M_h from $10^{10}h^{-1}\mathrm{M}_\odot$ to $5\times10^{12}h^{-1}\mathrm{M}_\odot$ is considered. If the source galaxies are more massive than $5\times10^{11}h^{-1}\mathrm{M}_\odot$, the contribution of intrinsic ellipticity correlations $C_{11}(\theta)$ becomes comparable to those observed. The intrinsic correlation $C_{22}(\theta)$ looks much smaller than the observation of Wittman et al. (2000), but the observed result is also significantly higher than the predictions of the LCDM model (cf. Wittman et al. 2000) for the lensing effect. We note that the intrinsic $C_{22}(\theta)$ for $M_h > 5\times10^{11}h^{-1}\mathrm{M}_\odot$ is comparable to the prediction of the LCDM model for the weak lensing.

In contrast to the previous studies of CM00 and HRH00, our results indicate that the intrinsic correlation of galaxy ellipticity can contribute significantly not only to shallow surveys but also to deep surveys. The difference of our conclusions from theirs stems from two causes. First, CM00 and HRH used the halos with more than 20 and 10 particles respectively to predict the angular correlations, which can lead to an underestimation of at least a factor of 2 as our convergence test showed. Second, we show that the ellipticity correlation increases with the halo mass, and the galaxy mass can be higher than the mass $2.8 \times 10^{11} h^{-1} \mathrm{M}_{\odot}$ adopted by CM00.

4 CONCLUSIONS

We used a set of high-resolution cosmological N-body simulations to study the intrinsic ellipticity correlation functions of halos. With the simulations of different resolutions, we found that the ellipticity correlations converge once the halos have more than 160 members. For halos with fewer members, the correlations are underestimated and the underestimation amounts to a factor of 2 when the halos have only 20 particles. After correcting for the resolution effects, we found that the ellipticity correlations of the halos in the bigger box ($L = 300\, h^{-1}$Mpc) agree very well with those obtained in the small box ($L = 100\, h^{-1}$Mpc). Combining these results from the different simulation boxes, we have presented accurate fitting formulae for the ellipticity correlation functions $c_{11}(r)$ and for the projected correlation functions $\Sigma_{11}(r_p)$ and $\Sigma_{22}(r_p)$ over a large range of halo mass (at least for $10^{10} \leqslant M_h \leqslant 10^{13} h^{-1} \mathrm{M}_{\odot}$). The latter two functions can be used to predict the contribution of the intrinsic correlations to deep lensing surveys. With reasonable assumptions for the redshift distribution of galaxies and for the mass of galaxies, we found that the intrinsic ellipticity correlation can contribute significantly not only to shallow surveys but also to deep surveys, if the galaxies have the same shapes as their host halos.

ACKNOWLEDGMENTS

The author would like to thank Gerhard Börner, Joe Silk and Simon White for useful discussions. The numerical simulations used in this paper were carried out at ADAC (the Astronomical Data Analysis Center) of the National Astronomical Observatory, Japan, and Yasushi Suto is thanked for his support at various stages of obtaining the simulation sample. The work is supported in part by the One-Hundred-Talent Program, by NKBRSF(G19990754), and by NSFC(No. 10125314).

REFERENCES

Bacon D., Refregier A., Ellis R., 2000, MNRAS, 325, 1065
Bacon, D., Massey, R., Refregier, A., & Ellis, R. 2002, MNRAS, submitted, astro-ph/0203134
Bartelmann, M., & Schneider, P. 2001, Physics Reports, 340, 291
Blandford R. D., Saust A. B., Brainerd T. G., Villumsen J. V., 1991, MNRAS, 251, 600
Brown M. L., Taylor A. N., Hambly N. C., Dye S., 2002, MNRAS, 333, 501
Catelan, P., Kamionkowski, M., & Blandford, R.D. 2001, MNRAS, 320, L7
Catelan, P. & Porciani, C. 2001, MNRAS, 323, 713
Crittenden, R.G., Natarajan, P., Pen, U.-L., & Theuns, T. 2001, ApJ, 559, 552
Crittenden R. G., Natarajan P., Pen U., Theuns T., 2002, ApJ, 568, 20
Croft, R. A. C. & Metzler, C. A. 2000, ApJ, 545, 561
Heavens, A., Refregier, A., & Heymans, C. 2000, MNRAS, 319, 649
Hoekstra, H., Yee, H. K. C., & Gladders, D. 2002a, astro-ph 0202285
Hoekstra, H., Yee, H. K. C., & Gladders, D. 2002b, astro-ph 0204295
Hui, L. & Zhang, J. 2002, astro-ph/0205512
Jing Y. P., 1998, ApJ, 503, L9
Jing Y. P., Suto Y., 1998, ApJ, 494, L5
Jing Y. P., Suto Y., 2002, ApJ, 574, in press; astro-ph/0202064
Kaiser, N. 1992, ApJ, 388, 272
Kaiser, N., Wilson, G. & Luppino, G. 2000, astro-ph 0003338
Lee, J., & Pen, U. 2000, ApJ, 532, L5
Lee J., Pen U., 2001, ApJ, 555, 106
Lee J., Pen U., 2002, ApJ, 567, L111
Mackey, J., White, M., & Kamionkowski, M. 2002, MNRAS, 332, 788
Maoli, R., Van Waerbeke, L., Mellier, Y., Schneider, P. Jain, B., Bernardeau, F., Erben, T. & Fort, B. 2001, A&A, 368, 766
Miralda-Escude J., 1991, ApJ, 380, 1
Mellier Y., 1999, ARAA, 37, 127
Pen U., Lee J., Seljak U. ;, 2000, ApJ, 543, L107
Pen U., Van Waerbeke L., Mellier Y., 2002, ApJ, 567, 31
Plionis M., 1994, ApJS, 95, 401
Porciani, C., Dekel, A. & Hoffman, Y. 2002, MNRAS, 332, 325
Schneider, P., van Waerbeke, L. & Mellier, Y. 2002, submitted to A& A, astro-ph 0112441
Smail I., Hogg D. W., Yan L., Cohen J. G., 1995, ApJ, 449, L105
Rhodes J., Refregier A., Groth E. J., 2001, ApJ, 552, L85
Rhodes J., Refregier A., Groth E. J., 2000, ApJ, 536, 79
Van Waerbeke L., Mellier Y., Erben T., et al., 2000, A&A, 358, 30
Van Waerbeke L., Mellier Y., Radovich M., et al., 2001, A&A, 374, 757
Wittman D. M., Tyson J. A., Kirkman D., Dell'Antonio I., Bernstein G., 2000, Nature, 405, 143